Annexin A2 depletion delays EGFR endocytic trafficking via cofilin activation and enhances EGFR signaling and metastasis formation

Graauw, M. de; Cao, L.; Winkel, L.; Miltenburg, M.H.A.M. van; Dévédec, S.E. le; Klop, M.; ... ; Water, B. van de

Oncogene (2014) **33,** 2610–2619

www.nature.com/onc

ORIGINAL ARTICLE

Annexin A2 depletion delays EGFR endocytic trafficking via cofilin activation and enhances EGFR signaling and metastasis formation

M de Graauw[1], L Cao[2,5], L Winkel[3,5], MHAM van Miltenburg[4], SE le Dévédec[1], M Klop[1], K Yan[2], C Pont[1], V-M Rogkoti[1], A Tijsma[1], A Chaudhuri[1], R Lalai[1], L Price[1], F Verbeek[2] and B van de Water[1]

Enhanced epidermal growth factor receptor (EGFR) activity has been strongly linked to breast cancer progression and mediators of EGFR endocytosis may well be involved. We developed a semi-automated high-content fluorescence microscopy-based EGFR endocytosis screen to identify proteins that mediate EGFR endocytosis in human HBL100 breast cancer cells. Knockdown of 172 individual endocytosis and actin-regulatory genes with small interfering RNAs led to the identification of 14 genes of which the contribution to EGFR endocytosis in breast cancer is until now poorly defined, including *DNAJC6*, *GDI2*, *FGD6*, *HAX1*, *NECAP2* and *AnxA2*. We show that depletion of the actin and endocytosis regulatory protein annexin A2 (AnxA2) in a panel of four triple negative breast cancer (TNBC) cell lines affected EGFR endocytosis. Depletion of AnxA2 in the aggressive and highly metastatic MDA-MB-231 TNBC cell line resulted in the inhibition of EGFR transport beyond the early endosomes. This inhibition coincided with enhanced epidermal growth factor (EGF)-induced cell migration and downstream signaling via c-Jun N-terminal kinase (JNK) and Akt. Moreover, AnxA2 knockdown increased lung metastasis formation in mice. The effect of AnxA2 knockdown on EGFR endocytosis in MDA-MB-231 was related to dephosphorylation/activation of the actin-severing protein cofilin, as re-expression of an inactive S3E-cofilin mutant, but not an active S3A-cofilin mutant, re-established EGFR endocytosis to control levels. Together, our data provide evidence for AnxA2 as a mediator of EGFR endocytosis and signaling in breast cancer via regulation of cofilin activation.

Oncogene (2014) **33,** 2610–2619; doi:10.1038/onc.2013.219; published online 24 June 2013

Keywords: AnxA2; breast cancer; EGFR; endocytosis; metastasis

INTRODUCTION

The epidermal growth factor receptor (EGFR) is important for normal growth and function of breast tissue and, when inappropriately activated, one of the main proteins involved in the development and progression of breast cancer.[1] A strong correlation has been found between the presence of high levels of EGFR in breast tumors and the aggressive potential of the tumor.[2] When EGFR is activated by binding to EGF, a chain of events is triggered. The EGFR dimerizes, which stimulates its intrinsic intracellular protein-tyrosine kinase activity, resulting in autophosphorylation of several tyrosine residues in the C-terminal domain of EGFR. Subsequently, different downstream signaling cascades are activated, including the Mitogen-activated protein kinase, JNK and Akt pathway. To prevent excessive growth and, thereby, formation of breast cancer, EGFR-dependent growth is, among others, controlled by endocytosis.[3]

EGFR endocytosis is a multistep process, including receptor internalization at the plasma membrane, sorting in early endosomes, transport to late endosomes, uptake in multi-vesicular bodies and degradation in the lysosomes.[4] As EGFR remains active within the endosomes until it is degraded, these endosomes can themselves form signaling platforms, resulting in propagation of intracellular signaling or in initiation of protein signaling cascades.[5] Over the past decades, many proteins have been shown to contribute to EGFR endocytosis, of which the adaptor protein growth factor receptor-bound Grb2 and the ubiquitin ligase Cbl have been described as two of the main regulators of EGFR endocytosis.[6,7]

It has long been known that overexpression, mutations, deletions and production of autocrine ligands contribute to aberrant activation of EGFR in breast cancer. Yet, increasing evidence shows that aberrant EGFR signaling in breast cancer cells may also be caused by defects in the receptor endocytosis and degradation route.[8] A defective endocytosis route may result in persistent localization and activation of EGFR at the plasma membrane of cancer cells, as internalization of the receptor into early endosomes may be blocked or inhibited.[5] In addition, EGFR that is taken up into early endosomes may continue to signal from these endosomes, as passage to late endosomes and to degradation lysosomes may not take place.[5] Together, this results in enhanced EGFR signaling promoting cancer cell proliferation, invasion and metastasis formation. A better mechanistic understanding of the proteins that control EGFR endocytosis and thereby signaling in breast cancer cells may shed light on the mechanisms that control EGFR endocytosis and signaling in breast cancer.

To identify regulators of EGFR endocytosis in breast cancer cells, we developed a semi-automated high-content fluorescent

[1]Division of Toxicology, LACDR, Leiden University, Leiden, The Netherlands; [2]Imaging and Bio-informatics group, LIACS, Leiden University, Leiden, The Netherlands; [3]Biomechanics Laboratory, Erasmus MC, Rotterdam, The Netherlands and [4]Department of Molecular Pathology, Netherland Cancer Institute, Amsterdam, The Netherlands. Correspondence: Dr B van de Water or Dr M de Graauw, Division of Toxicology, LACDR, Leiden University, Einsteinweg 55, PO Box 9502, 2300 RA, Leiden, The Netherlands. E-mail: b.water@lacdr.leidenuniv.nl or m.de.graauw@lacdr.leidenuniv.nl
[5]These authors contributed equally to this work.
Received 18 April 2013; revised 19 April 2013; accepted 14 May 2013; published online 24 June 2013

microscopy-based RNA interference (RNAi) screen with subsequent automated image analysis. A dedicated library of small interference RNAs (siRNAs) targeting 172 regulators of endocytosis and actin dynamics was used and the siRNAs were screened for their ability to alter endogenous EGFR endocytosis in the HBL100 breast cancer cell line. We identified 14, of which the contribution to EGFR endocytosis in breast cancer is until now poorly defined. We evaluated the role of one of these genes, AnxA2, in breast cancer progression in further detail. Together, our data provide evidence for a novel role of AnxA2 in EGFR endocytosis, signaling and metastasis formation via activation of cofilin.

RESULTS

RNAi screen to identify EGFR endocytosis regulators in breast cancer cells

To identify proteins that regulate EGFR endocytosis in human breast cancer cells, we developed a semi-automated high-content fluorescence microscopy-based RNAi screen that allows quantitative analysis of EGFR endocytosis in breast cancer cells (Supplementary Figure 1A). On basis of their homogeneous and consistent EGFR endocytosis profile, we selected the EGFR positive, mildly transformed HBL100 breast cancer cell line for our screen. EGF treatment of HBL100 cells resulted in internalization of the EGFR (Figure 1a). Over time, the number of EGFR-positive endosomes per cell increased and the amount of EGFR localized at the plasma membrane decreased, which was quantified using our previously developed image analysis algorithms for EGFR endocytosis[9] (Figure 1b and Supplementary Figure 1B). EGFR internalization was associated with signaling via Akt and ERK1/2 (extracellular regulated MAP kinase) as determined by western blotting (Figure 1c).

Next, we set up siRNA-mediated knockdown by transfecting HBL100 cells with non-targeting siRNA (siRNA control (siCtrl) and siRNA green fluorescent protein (siGFP)) and siRNA-targeting EGFR (Figures 1d and e). Cells were exposed to EGF for 60 min to allow complete endocytic uptake of EGFR. At 60 min of EGF exposure, the average number of endosomes per cell was not significantly different between non-treated, siCtrl#2 and siGFP, allowing the use of these controls for siRNA screening (Figures 1d and e, Supplementary Figure 1C). Moreover, transfection of HBL100 cells with a siRNA SmartPool-targeting EGFR resulted in a ~90% knockdown of EGFR (Figures 1d and e). Together, these data demonstrate the feasibility of siRNA-mediated knockdown in HBL100 cells and quantification of EGFR endocytosis based on fluorescent staining and confocal microscopy imaging.

Next, a dedicated library consisting of 172 siRNAs targeting known endocytosis and actin regulators (Supplementary Table 1)

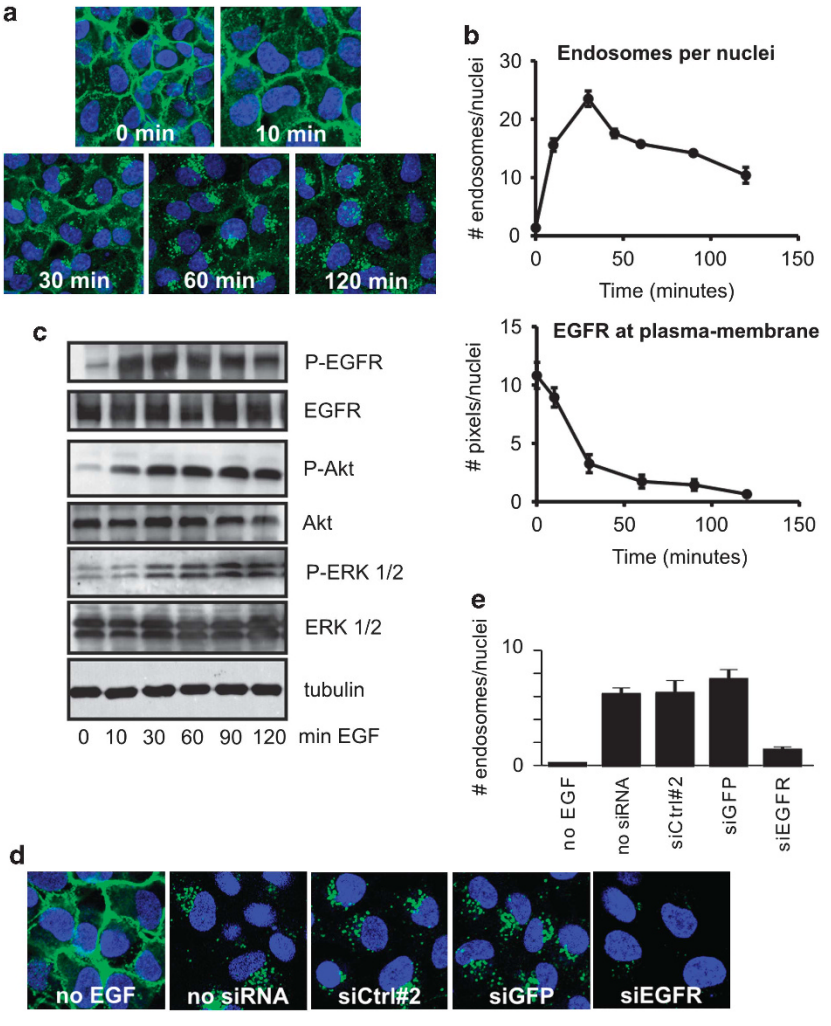

Figure 1. EGFR endocytosis in HBL100 breast cells. HBL100 cells were exposed to EGF (50 ng/ml) for indicated time points, fixated and stained for EGFR and Hoechst (**a**). The number of endosomes and EGFR localization at the plasma membrane was quantified (**b**). EGFR downstream signaling was determined using western blotting (**c**). HBL100 cells were transfected using Dharmacon Smartpool siRNAs (siCtrl, siGFP, siRNA-targeting EGFR (siEGFR)) or none treated. At day 3, cells were exposed to 50 ng/ml EGF for 60 min, fixated and stained for EGFR and Hoechst. Cells were imaged using confocal laser scanning microscopy (**d**). The number of endosomes was quantified (**e**).

was used to determine the role of these target genes in EGFR endocytosis in human breast cancer cells. This library included known as well as unknown EGFR mediators. The screen was performed in duplicate and each a 96-well plate included five duplicate control wells, including untreated cells, EGF-treated cells either untransfected or transfected with siCtrl, siGFP or siRNA-targeting EGFR (Supplementary Figure 1). Within and between the different 96-well plates used for screening, no significant differences were observed between no siRNA, siCtrl and siGFP, whereas siRNA-targeting EGFR treatment resulted in 85–90% knockdown in all wells (Supplementary Figures 1C and 2). Only those siRNAs of which knockdown affected EGFR endocytosis in both screens and resulted in significantly ($P<0.05$) different numbers of EGFR-positive endosomes compared with no siRNA, siCtrl as well as siGFP conditions were selected as positive hits (Figures 2a, $n=61$). These EGFR endocytosis mediators included transport proteins, members of the (Rho)GTPase, members of the Ras superfamily, PI-3K family members and annexin family members (Supplementary Table 2).

For 24 hits, information on their role in EGFR endocytosis was scarce. To validate these primary hits, a deconvolution secondary screen was performed in which the four duplexes from each of the 24 SMARTpool hits were individually screened (Supplementary Table 3). From the 24 primary hits, NECAP2 and AnxA2 were validated with all four individual siRNAs and 12 primary hits were validated by three out of four individual siRNAs (Figure 2b and Supplementary Figures 3 and 4). Primary hits that were validated by less than three individual siRNAs were not considered as high confidence hits. Thus, using semi-automated high-content fluorescence microscopy-based RNAi endocytosis screening, we successfully identified a set of novel regulators of EGFR endocytosis in HBL100 breast cancer cells that are of interest for further study.

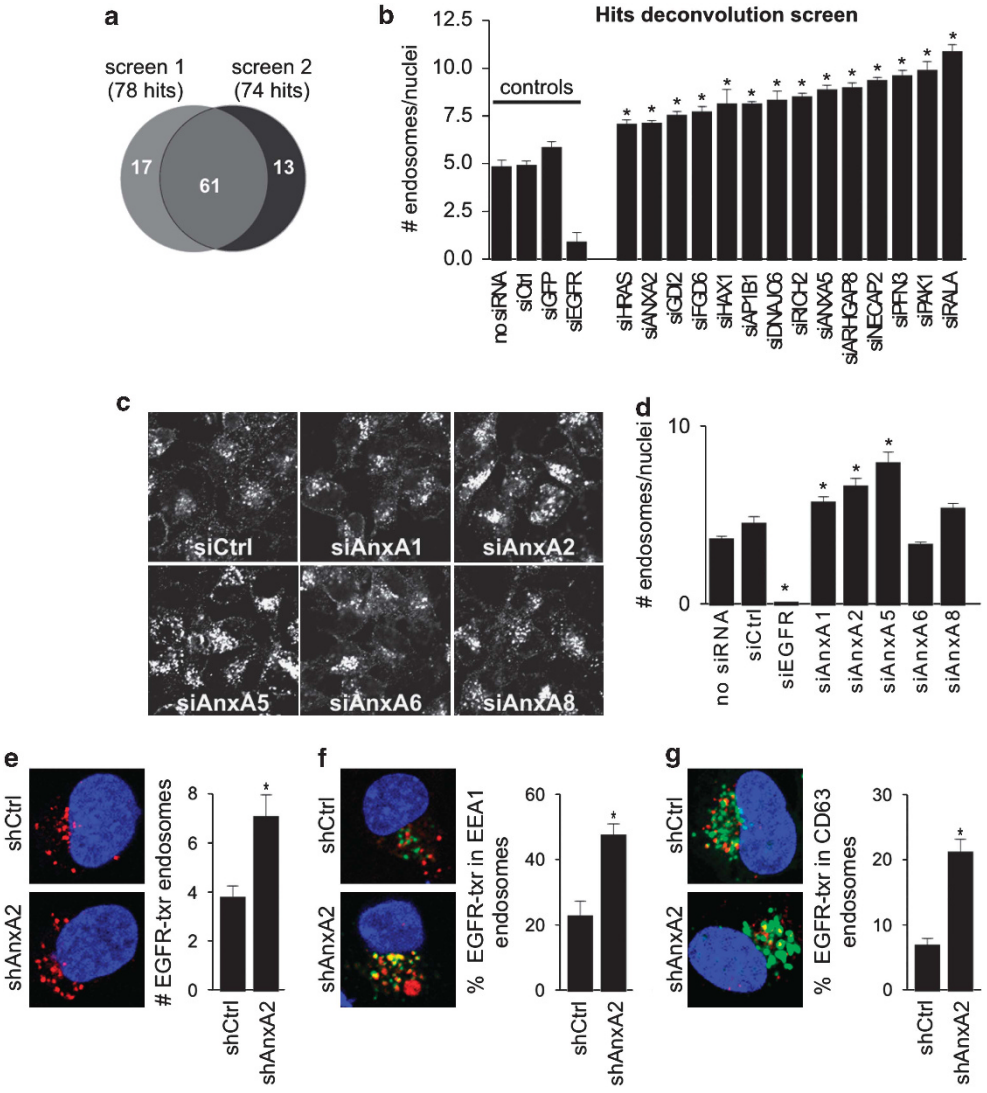

Figure 2. RNA interference screen identifies EGFR endocytosis regulators in HBL100 cells. RNA interference screening was performed as described in Materials and methods. In total, 61 genes were identified, of which knockdown significantly affected EGFR endocytosis (**a**). Twenty-four primary hits were validated using four individual siRNAs, confirming 14 proteins (**b**). HBL100 cells were transfected using Dharmacon Smartpool siRNAs directed against AnxA1, A2, A5, A6 and A8, exposed to 50 ng/ml EGF for 60 min, fixated and stained for EGFR and Hoechst. Cells were imaged using confocal laser scanning microscopy (**c**) and the number of endosomes was quantified (**d**). AnxA2 knockdown in HBL100 cells was established using lenti-viral shRNA specific for AnxA2 (shAnxA2) and a scrambled sequence (shCtrl). Cells were exposed to EGF-txr (red) for 60 min (**e**), 30 min (**f**) and 90 min (**g**) and co-stained with EEA1 (green) or CD63 (green). The percentage of EGF-txr in EEA1-positive early endosomes or CD63-positive late endosomes was determined. * denotes $P<0.05$.

AnxA2 differentially regulates EGFR endocytosis in mild and aggressive breast cancer cells

The annexin family can provide an anchor between the actin cytoskeleton and the endosomal membranes[10] and therefore represents a somewhat novel class of EGFR endocytosis regulators. Our screen identified AnxA1, A2 and A5 as mediators of EGFR endocytosis (Figures 2c and d). We have previously shown the involvement of AnxA1 in triple negative breast cancer (TNBC) progression.[11] Here we investigated the role of its close family member AnxA2 in breast cancer progression in further detail.

To determine whether AnxA2 knockdown increased the number of EGFR-positive endosomes in other EGFR-positive breast cancer cell lines as well, we generated stable AnxA2 knockdown cell lines using lenti-viral small hairpin RNA (shRNA) transduction of five EGFR-positive breast cancer cell lines (for example, HBL100, MDA-MB-231 wild-type (WT), MDA-MB-231 LM2 subclone of Massague *et al*.,[12] MDA-MB-157 and BT549 cells). Compared with shCtrl cells, all shAnxA2 cells showed an increased number of EGFR-positive endosomes upon stimulation of cells with EGF or EGF-txr (texas-red) (Figures 2e, 3a–c, Supplementary Figure 5).

Although all five breast cancer cell lines are EGFR positive, differences are apparent at both the genetic and phenotypic level. Although the HBL100 cell line is mildly transformed and non-metastatic, the other four belong to the more aggressive, TNBC subtype, of which the MDA-MB-231 LM2 subclone of Massague *et al*.[12] is a most often used and highly metastatic cell line. Given these differences we reasoned that the mechanisms underlying the increase in EGFR-positive endosomes may differ between the mildly transformed, non-metastatic HBL100 cell line and the more aggressive, metastatic MDA-MB-231 LM2 cell line. Therefore, we determined the percentage of EGF-txr in EEA1-positive early endosomes or in CD63 late endosomes to verify whether the increase in the number of EGFR-positive endosomes was due to enhanced EGFR uptake or inhibition of EGFR transport beyond the early endosomes EGF exposure of shAnxA2 HBL100 cells resulted in an increase in the percentage of EGF-txr localizing in the EEA1-positive early endosomes at 30 min of exposure (Figure 2f) and an increase in the percentage of EGF-txr in CD63-positive late endosomes at 90 min after exposure (Figure 2g). Thus, EGFR uptake and endocytic transport seems to be more rapid in shAnxA2 HBL100 cells compared with shCtrl HBL100 cells. In contrast to HBL100 cells, at 10 min of EGF-txr exposure no significant difference in the percentage of EGF-txr in EEA1-positive early endosomes was observed between WT, shCtrl and shAnxA2 MDA-MB-231 LM2 cells, indicating that EGFR uptake followed by processing is not increased upon knockdown of AnxA2 in MDA-MB-231LM2 cells (Figure 3d). Over time, the percentage of EGF-txr in EEA1-positive early endosomes decreased in WT and shCtrl, but remained constant in shAnxA2 cells (Figures 3d and e). This coincided with a reduced percentage of EGF-txr in CD63-positive late endosomes in these cells (Figures 3f and g). Together, these data indicate that AnxA2 knockdown reduced the transport of EGFR beyond the early endosomes in MDA-MB-231 LM2 cells, which is in contrast to the effect of AnxA2 knockdown in the mildly transformed HBL100 cells, suggesting a different role for AnxA2 in EGFR regulation in mildly versus more aggressive breast cancer cell lines

AnxA2 depletion in MDA-MB-231 cells results in enhanced EGF-induced migration and signaling

Monoclonal anti-AnxA2 treatment has previously been shown to inhibit migration of MDA-MB-231 cells.[13] Therefore, we next tested whether shRNA-based knockdown would also inhibit MDA-MB-231 cell migration. Indeed, depletion of AnxA2 resulted in reduced random cell migration (Figure 4a). Similar observations were made for the mildly transformed HBL100 cell line (Supplementary Figure 6A). Yet, shAnxA2 MDA-MB-231 cells were significantly more sensitive toward EGF-induced cell migration compared with shCtrl cells (Figure 4b), indicating that knockdown of AnxA2 resulted in enhanced EGF-induced cell migration. In contrast, EGF-induced cell migration was inhibited in shAnxA2 HBL100 cells (Supplementary Figure 6B). This difference in response to EGF may be explained by the difference in contribution of AnxA2 to EGFR endocytosis between these mildly and highly aggressive breast cancer cell lines. In addition, cells were grown in a three-dimensional collagen microenvironment in the presence of EGF (Supplementary Figure 7) and growth behavior was quantified using our novel imaging analysis approach (Zi *et al.* in preparation). Principal component analysis showed a significant difference between cell growth behavior of shAxA2 cells compared with shCtrl cells, of which shAnxA2 obtained a more invasive phenotype.

EGFR that is taken up into early endosomes may continue to signal from these endosomes.[5] As knockdown of AnxA2 delayed EGFR endocytosis in MDA-MB-231 cells, we hypothesized that the enhanced response toward EGF-induced migration may be explained by enhanced EGFR signaling in AnxA2-depleted MDA-MB-231 cells. Therefore, MDA-MB-231 LM2 cells were exposed to EGF over time and downstream signaling was determined using western blot analysis. Knockdown of AnxA2 resulted in increased phosphorylation of the EGFR itself and enhanced downstream signaling via the Akt and JNK pathway (Figures 4c and d). Signaling via the ERK pathway was not affected. In conjunction with the reduced response toward EGF-induced migration in HBL100 cells, EGFR downstream signaling was reduced in HBL100 shAnxA2 cells (Supplementary Figures 6C and D). Even though EGFR endocytosis was delayed at early time points in MDA-MB-231 cells, EGF-induced EGFR endocytosis was not completely blocked and degradation could still take place (Figures 4e and f).

AnxA2 knockdown increases metastasis formation of the TNBC MDA-MB-231 cell line

Enhanced EGFR expression and activation has been associated with enhanced breast cancer progression.[1] As AnxA2 knockdown stimulates EGFR signaling in MDA-MB-231 cells *in vitro*, we anticipated that AnxA2 knockdown would enhance formation of lung metastasis *in vivo*. To determine the effect of AnxA2 knockdown *in vivo*, we established a mouse model for TNBC using the MDA-MB-231 GFP/luc subclone of Massague *et al*.[12] MDA-MB-231 WT, shCtrl and shAnxA2 cell lines were injected into the mammary fat pads of 12-week-old Rag2$^{-/-}\gamma c^{-/-}$ mice (Figure 5). Knockdown of AnxA2 did not alter primary tumor growth and cell proliferation as determined by ki67 staining of the primary tumor (Figures 5a and b). Animals were killed at day 17 (shCtrl and shAnxA2) and day 21 (WT) after removal of the primary tumor and AnxA2 knockdown in the primary tumors was confirmed using immunostaining for AnxA2 (Figure 5b). Bio-luminescent imaging of the lungs showed that depletion of AnxA2 enhanced total lung tumor burden (Figure 5c). To quantify the number and size of the lung metastasis in more detail, lung sections were stained for hematoxylin/eosin to visualize lung metastasis (Figure 5d). Depletion of AnxA2 resulted in a significant increase in the number of lung metastasis (Figure 5e), but did not change the average size of the metastases (Figure 5f). Similar findings were obtained for another highly aggressive TNBC cell line, the metastatic rat MTLn3 cell line, which is also positive for EGFR (Supplementary Figure 8). Together, these data indicate that the EGFR endocytosis regulator AnxA2, which was identified in our RNAi EGFR endocytosis screen, mediates the metastasizing capacity of EGFR-positive MDA-MB-231 cells.

Cofilin is activated upon depletion of AnxA2 and reconstitution of inactive cofilin re-establishes EGFR endocytosis

We have previously shown that AnxA2 is able to regulate cofilin phosphorylation and thereby its activity in MDCK cells.[14] As cofilin

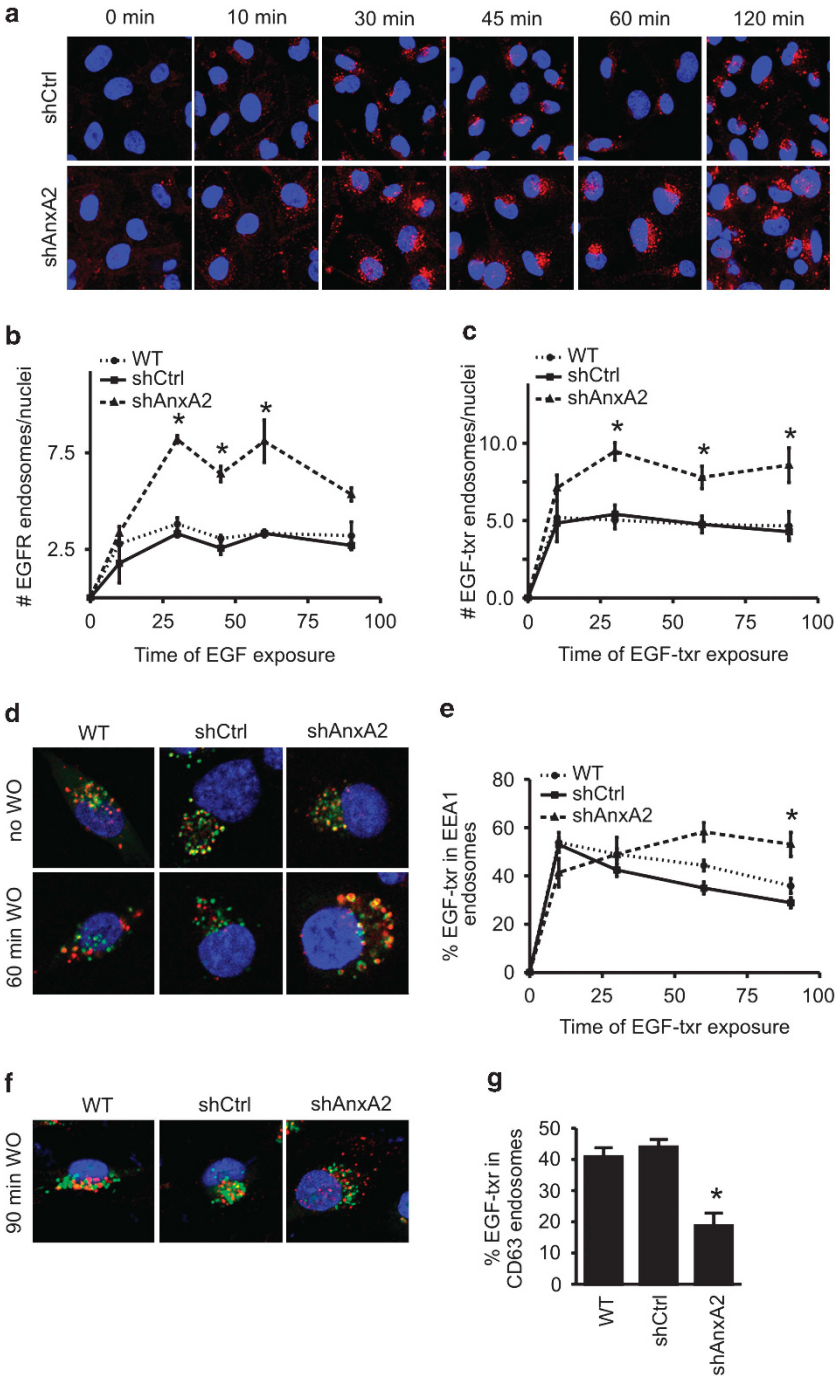

Figure 3. AnxA2 inhibits transport of EGFR beyond early endosomes. AnxA2 knockdown in MDA-MB-231 was established using lenti-viral shRNA specific for AnxA2 (shAnxA2) and a scrambled sequence (shCtrl). Cells were exposed to 50 ng/ml EGF (**a**) or 100 ng/ml EGF-txr for indicated time points, fixated, stained for EGFR and Hoechst (**a**) and quantified for EGFR (**b**) and EGF-txr (**c**) endocytosis over time. EGF-txr-exposed cells were co-stained for the early endosome marker EEA1 (**d**) and the percentage of EGF-txr (red) in EEA1 (green)-positive endosomes was determined over time (**e**). In addition, EGF-txr (red)-exposed cells were co-stained for the late endosome marker CD63 (green) (**f**) and the percentage of EGF-txr in CD63-positive endosomes was determined over time (**g**). * denotes $P < 0.05$. WO, wash-out.

is known to mediate endocytosis,[15,16] we determined whether AnxA2 affected EGFR endocytosis via its effect on cofilin activation. Depletion of AnxA2 in the human MDA-MB-231 BLBC cell line resulted in dephosphorylation and thereby activation of cofilin both in the presence and absence of serum (Figures 6a and b). Although EGF exposure has been shown to result in cofilin phosphorylation in NIH3T3 cells,[17] no increase in cofilin phosphorylation was observed in EGF-exposed MDA-MB-231 cells (Figure 6c). To determine whether the decrease in cofilin phosphorylation was associated with the delay in EGFR endocytosis, shAnxA2 cells were transiently transfected with either a phospho-mimicking (S3E) or a phospho-defective (S3A) cofilin mutant and thereafter treated with EGF to induce EGFR endocytosis. Expression of the phospho-mimicking,

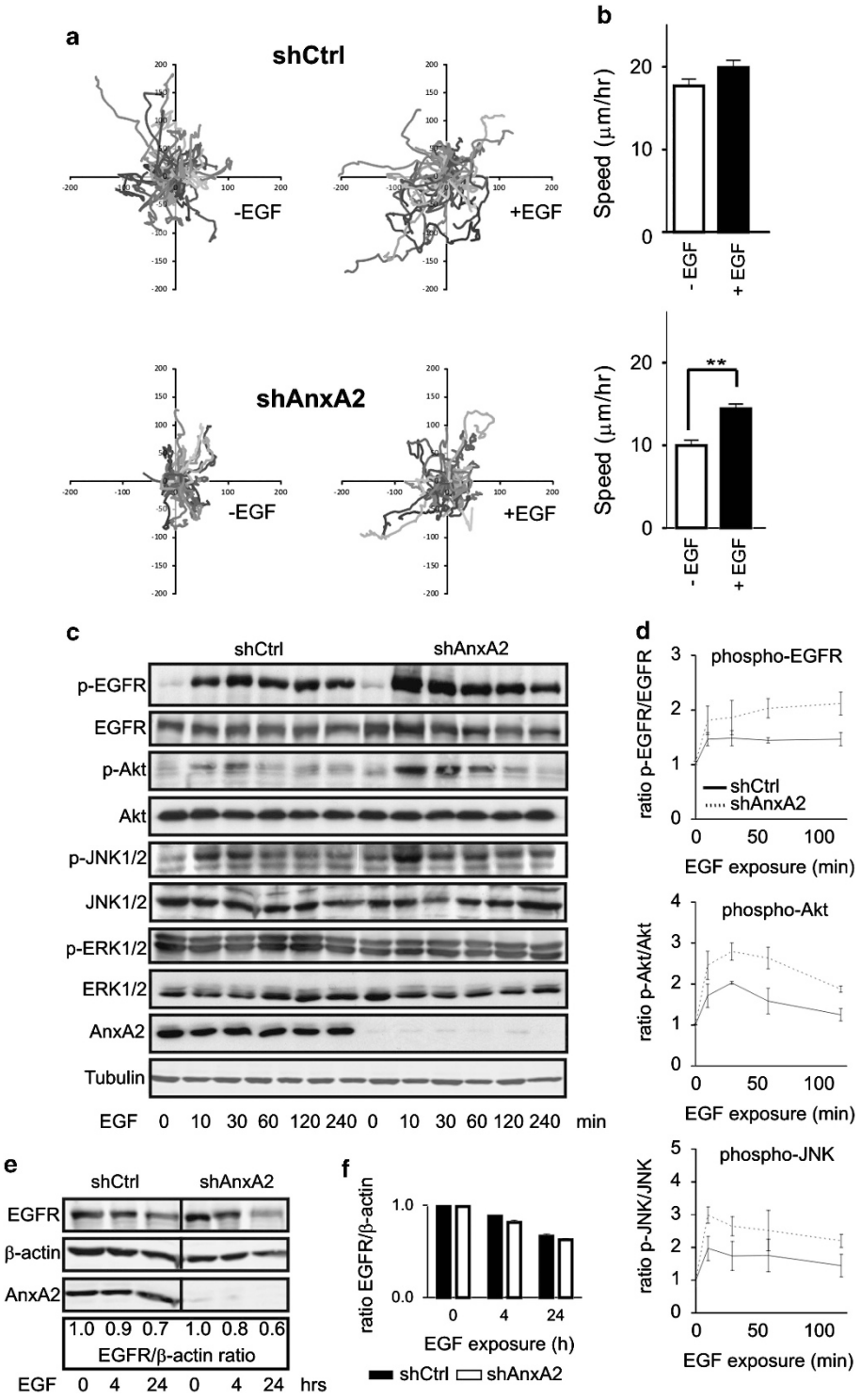

Figure 4. AnxA2 knockdown enhances EGF-induced cell migration and signaling in MDA-MB-231 cells. A random cell migration assay was performed in duplicate (four movies per experiment) in the absence and presence of 10 ng/ml EGF using shCtrl as well as shAnxA2 MDA-MB-231 LM2 cells to determine the effect of AnxA2 knockdown on cell migration. Cell migration trajectories are depicted in **a** and average speed was quantified using tracking of the cells with differential interference contrast/Hoechst (**b**).The effect of AnxA2 knockdown on EGFR-dependent signaling was determined using western blotting of EGF-exposed cells for phospho-EGFR, phospho-Akt, phospho-ERK and phospho-JNK (**c**). Total EGFR, Akt, JNK and ERK were used to quantify the levels of protein phosphorylation (**d**). To determine whether EGF-induced EGFR degradation can still take place, cells were stimulated with EGF in the presence of cyclohexamide (10 μg/ml) to inhibit protein synthesis for 4 and 24 h. Cell lysates were generated in triplicate and analyzed for EGFR expression using western blot analysis (**e**), which was quantified in **f**. * denotes $P < 0.01$. d, day.

inactive cofilin mutant (S3E), but not the phospho-defective, active cofilin mutant (S3A) decreased the number of EGFR-positive endosomes in shAnxA2 to the levels of shCtrl cells (Figures 6d and e). Together, these data suggest that AnxA2 mediates EGFR endocytosis via regulation of the actin severing protein cofilin.

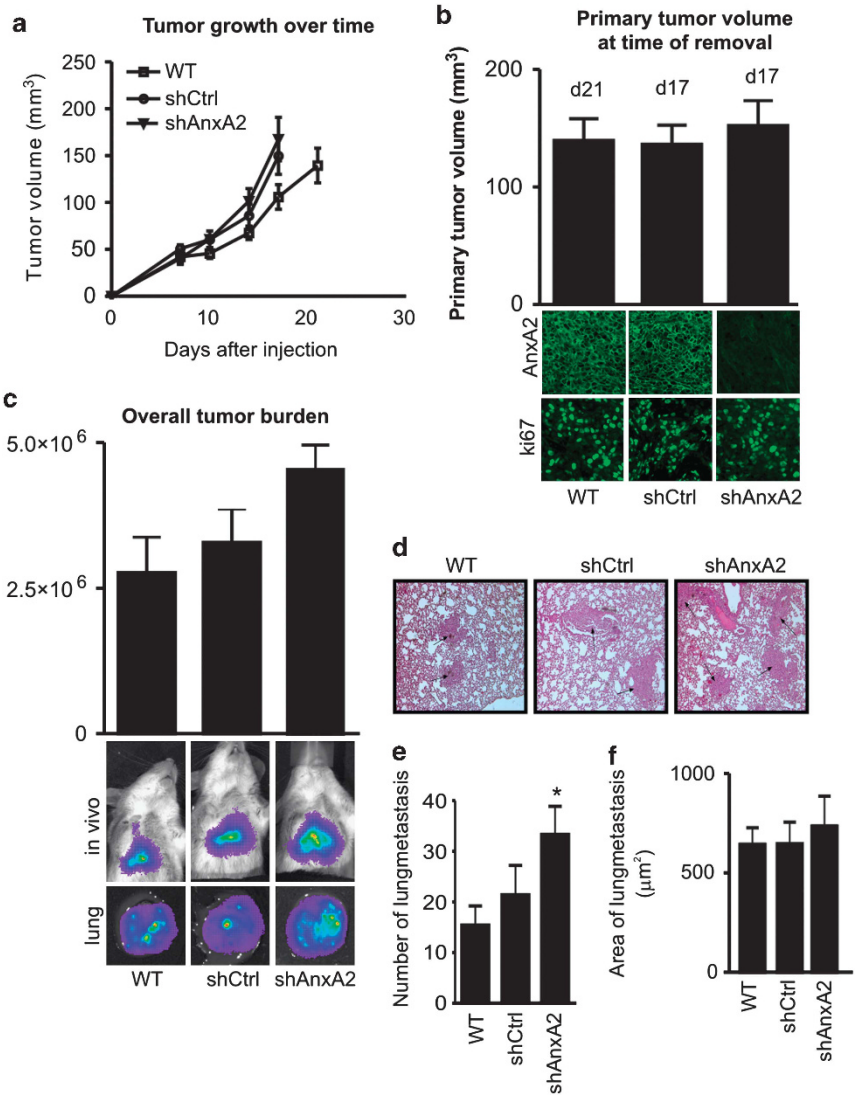

Figure 5. AnxA2 depletion increased metastatic spread of MDA-MB-231 cells in mice. MDA-MB-231 LM2 cells expressing GFP and Luc were transduced with lenti-viral shRNA specific for turboGFP (control shRNA) or AnxA2. Cells were injected into the mammary fat pad of 12-week-old Rag2$^{-/-}$/c$^{-/-}$ mice. Primary tumor volume was measured over time (**a**) and at 17–26 days after injection, mice were killed. Primary tumor volume as well as AnxA2 and ki67 proteins expression levels were determined (**b**). Lung metastasis formation was determined using luminesence imaging (**c**) and hematoxylin-eosin (HE) staining (**d**). Total lung burden (**c**) and the individual lung metastasis number (**e**) and size (**f**) were quantified. * denotes $P<0.05$.

DISCUSSION

To identify novel mediators of EGFR endocytosis in human breast cancer cells, we developed a semi-automated high-content imaging-based endocytosis assay with automated image analysis. We identified 61 proteins that mediated EGFR endocytosis in human breast cancer cells, and validated 14 out of 24 proteins, for which information on their role in EGFR endocytosis was scarce.

The 14 EGFR regulators that were validated using four individual siRNAs, included actin regulatory proteins like RICH2 and FGD6. Although their family members have been associated with cdc42 activation,[18,19] their function in relation to EGFR endocytosis has yet to be determined. In addition, our screen resulted in identification of proteins known to be involved in endocytosis (for example, HAX1, DNAJC6, NECAP2), but their association with EGFR endocytosis in breast cancer remains thus far unknown. A somewhat novel class of EGFR endocytosis regulators are proteins that can interact with both the actin cytoskeleton and the endosomal membranes, including annexin proteins.[10] This ability to interact with both the actin cytoskeleton as well as the endosomes provides a rather unique mechanism by which annexins could mediate EGFR endocytosis.

Our screen identified AnxA1, AnxA2 and AnxA5 as potential mediators of EGFR endocytosis. Previously, AnxA1, AnxA6 and AnxA8 have been linked to EGFR endocytosis in various cell types.[20–22] As AnxA6 is not expressed in HBL100 cells,[21] knockdown of this gene did not result in significant changes in the number of endosomes. Moreover, although knockdown of AnxA8 increased the number of endosomes (Figures 2c and d), this was only significant compared with two out of three control conditions (no siRNA and siCtrl). AnxA1 was one of the first EGFR substrates identified and interacts with the adaptor protein Grb2.[20,23] It is involved in EGF-induced multi-vesicular body biogenesis, in particular in inward vesicle budding of EGFR containing perimeter multi-vesicular body membranes.[24]

Increased expression of AnxA2 has been reported in numerous tumors.[25–27] Although enhanced EGFR signaling has been associated with these types of cancer, a functional role for

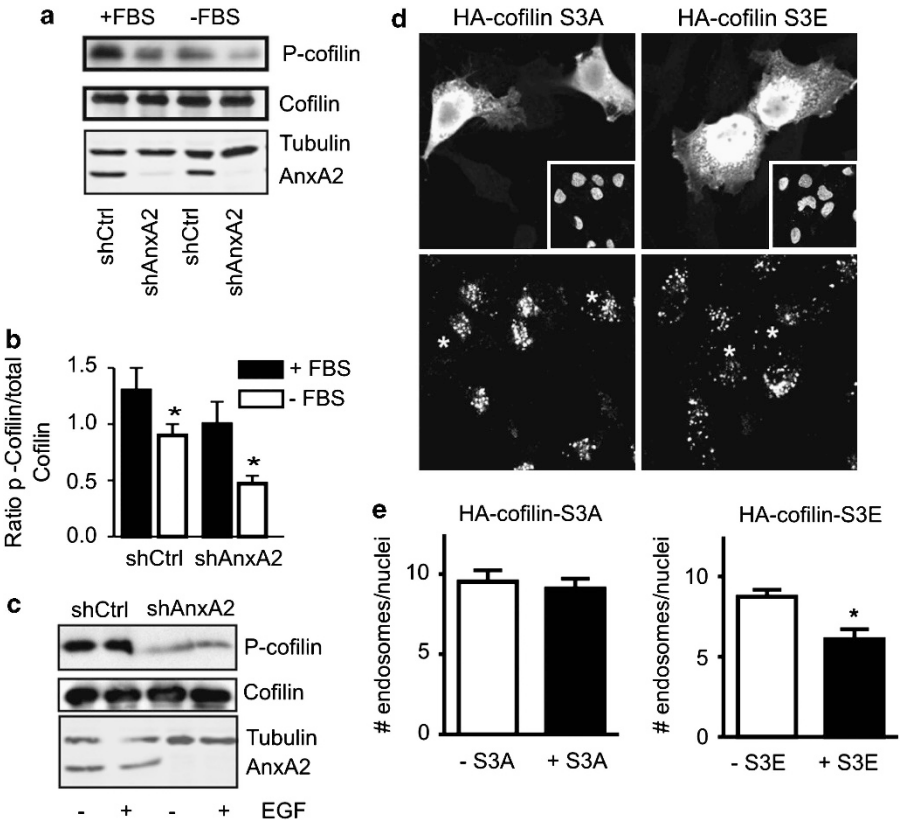

Figure 6. Knockdown of AnxA2 results in cofilin dephosphorylation, which is associated with the delay in EGFR endocytosis. Cells were analyzed for cofilin phosphorylation in the presence or absence of serum (**a**) using western blot analysis for cofilin, phosho-cofilin, tubulin and AnxA2. The phosphorylation levels of cofilin were quantified and expressed as a ratio of p-cofilin/cofilin (**b**). Exposure to 50 ng/ml EGF did not result in changes in the phosphorylation status of cofilin (**c**). Cells were transiently transfected with HA-S3A- or HA-S3E-cofilin (**d**) and the number of EGFR-positive endosomes per nuclei was determined (**e**). FBS, fetal bovine serum. * denotes $P<0.05$.

AnxA2 in the regulation of EGFR activity has not been described. Many different breast cancer subtypes have become apparent over the last years, each with their own genetic background and clinical outcome. Using a selection of different breast cancer cell lines, we show that depletion of AnxA2 enhanced EGFR endocytosis in the mildly transformed, non-metastatic HBL100 cell line, whereas it inhibited EGFR transport beyond the early endosomes in the more aggressive and highly metastatic MDA-MB-231 TNBC cell line. The inhibition of EGFR endocytosis is consistent with previous findings showing that AnxA2 is present on early endosomes[28,29] and that upon AnxA2 knockdown, EGF-txr accumulated in these early endosomes.[30]

As anticipated, the delay in EGFR endocytosis upon AnxA2 depletion in MDA-MB-231 cells was associated with enhanced EGFR signaling (Figure 5) via Akt and JNK and EGF-induced migration. These data fit with the current thinking that EGFR can still signal from the early endosomes.[5] In contrast, EGF-induced migration and signaling were reduced in the mildly transformed HBL100 cells. Thus, our data indicate a clear role for AnxA2 in EGFR endocytosis and related signaling events, but the outcome depends on the cellular context. Associated with our results are the findings of Shetty *et al.*[31] showed an important role for AnxA2 in the HER2+ breast cancer subtype. In addition, they showed that AnxA2 knockdown in the MDA-MB-231 wt cell line resulted in decreased EGFR signaling via Src, p38, ERK and Stat3. These data are in contrast with our own findings obtained in the MDA-MB-231 LM2 subclone and may be explained by the fact that inactivation of these signaling pathways could be independent of the effect of AnxA2 on EGFR endocytosis or attributed to the genetic background of the MDA-MD-231 cell line used and/or the knockdown efficiency obtained in their studies. Current understanding indicates a pivotal role for enhanced EGFR signaling in breast cancer metastasis, mediated by enhanced EGF levels in the tumor microenvironment provided by tumor-associated macrophages.[32,33] Our data fit with this concept: *in vitro* two-dimensional and three-dimensional EGF enhances migration and invasion of shAnxA2 BC cells and *in vivo* local EGF is the likely to be driver of enhanced metastasis of these shAnxA2 BC cells.

The delay in EGFR endocytosis upon knockdown of AnxA2 in the MDA-MB-231 LM2 cell line was associated with dephosphorylation of cofilin as overexpression of a phospho-mimicking S3E mutant re-established EGFR endocytosis (Figure 6). We have previously shown that AnxA2 can influence cofilin phosphorylation in MDCK cells.[14] Yet, here AnxA2 depletion resulted in increased cofilin phosphorylation, suggesting that the effect of AnxA2 depletion is cell- or tissue-type dependent. Moreover, AnxA2 has been associated with upstream components of the cofilin pathway.[34,35] It remains elusive whether AnxA2 influences cofilin phosphorylation directly via competition of binding to actin monomers or via other mechanisms.

In contrast to our findings, expression of dominant negative LIMK, the upstream kinase that phosphorylates cofilin, or a S3A cofilin mutant in WT MDA-MD-231 cells resulted in efficient EGF-texas red transport.[36] Thus, although cofilin clearly contributes to EGFR endocytosis, the mechanism by which cofilin affects EGFR endocytosis may be dependent on other proteins, such as AnxA2. Interestingly, cofilin has been described as one of the driving forces for metastasis formation of EGFR-positive breast cancer cells.[37,38] Given the importance of cofilin in the control of breast

cancer progression, our data therefore suggest that AnxA2 may regulate TNBC progression via its effect on cofilin.

In conclusion, using a RNAi EGFR endocytosis screen, the actin and endosome-binding protein AnxA2 were identified as the mediator of EGFR endocytosis, signaling and breast cancer progression by controlling the phosphorylation status of the actin-severing protein cofilin.

MATERIALS AND METHODS

Antibodies

Anti-AnxA2 (BD Transduction Laboratories, Breda, The Netherlands, 610068), anti-estrogen receptor (Santa Cruz, Heidelberg, Germany, Sc-543), anti-Tubulin (Sigma-Aldrich, Zwijndrecht, The Netherlands, T-9026), anti-phospho-Tyr1173-EGFR (Cell Signaling, Bioke, Leiden, The Netherlands, 4407) anti-EGFR (Cell Signaling, 2232), anti-phospho-Thr202/Tyr204-MAPK (P-ERK; Cell Signaling, 9101), anti-MAPK p44/42 (ERK1/2; Cell Signaling, 4695), anti-phosphoSer473-Akt (Cell Signaling, 9271), anti-Akt (Cell Signaling, 9272), anti-Phospho-Thr183/Tyr185-SAPK/JNK (Cell Signaling, 9251), anti-SAPK/JNK (Cell Signaling, 9252), anti-beta-actin (Santa Cruz, sc-47778), anti-CD63 was obtained from Dr Neefjes, NKI, Amsterdam.

Cell line maintenance and treatments

Human breast cancer cell lines were kindly provided by Dr F Foekens (Erasmus MC) and tested for authenticity by Short Tandem Repeat in June 2012. MTLn3 rat mammary adenocarcinoma cells were cultured as described previously.[39] MDA-MB-231 LM2 clone (417-5) was generated as described previously[12] and kindly provided by Dr J Massague. Cells were grown in medium specified by the American Type Culture Collection at 37 °C under 5% CO_2 (culture media from GIBCO, Invitrogen, Grand Island, NY, USA). Real-time PCR analysis for these cell lines was performed as described previously.[40]

siRNA screen for EGFR endocytosis

An siRNA library targeting 172 endocytosis and actin regulatory genes was custom ordered (Dharmacon RNA Technologies, Fisher Scientific, Landsmeer, The Netherlands) and received in a 96-well format. HBL100 cells were plated (15 000 per well) and after 24 h transfected according to the manufactures protocol using a pool of four siRNA oligonucleotides (50 nM) combined with Dharmacon IV transfection reagent. After 24 h medium was refreshed. At day 2 after transfection, cells were serum starved for 4 h and thereafter treated with 50 ng/ml EGF for 60 min. Cells were fixated in formaldehyde and stained and imaged as described below.

Immunofluorescence microscopy

Immunofluorescence was performed as described previously.[41] Cells were exposed to EGF-texas red (txr) and/or stained with anti-EGFR, anti-EEA1, anti-CD63 overnight at 4 °C and subsequently incubated with Alexa-488-conjugated secondary antibody (Molecular Probes, Life Technologies Europe BV, Bleiswijk, The Netherlands) in combination with Hoechst. Image acquisition was performed using a Nikon TE2000 combined with a Prior stage and controlled by NIS Element Software.

Live cell imaging random cell migration assay

Cell migration was determined as described previously.[42] Three positions per well were automatically defined and the differential interference contrast and Hoechst signals were acquired with a CCD camera (pixel size: 0.64 μm) every 20 min for a total imaging period of 12 h using NIS software (Nikon, Amsterdam, The Netherlands).

Image analysis

For image analysis, raw microscopy images were converted into phenotype measurements that represented EGFR endocytosis-related phenomena using our previously developed automated image analysis for EGFR endocytosis.[9] The data analysis used these measurements to train a classifier through hierarchical classification strategy. The classifier categorized the endosome-objects into different phenotypic episodes. The best classifier was obtained for the number of EGFR-positive endosomes. For each well, the number of endosomes per nucleus was calculated. The Kolmogorov–Smrinov test was used to identify significant changes in the number of EGFR-positive endosomes per nucleus for different siRNAs compared with three controls (no siRNA, siCtrl, siGFP).

Stable knockdown of AnxA2

For preparation of stable shRNA cell lines, MDA-MB-231 cells were transduced with lentiviral shRNA vectors raised against human AnxA2 (5′-CCGGCTGTACTATTATATCCAGCAACTCGAGTTGCTGGATATAATAGTACAG TTTTTG-3′) and a non-targeting control vector (Sigma-Aldrich, collaboration with dr Hoeben, LUMC). Mtln3 cells were transduced using lenti-viral shRNA vectors raised against TurboGFP (shCtrl) and rat AnxA2 (Open Biosystems, Fisher Scientific, Landsmeer, The Netherlands, TRCN000011068). Cells were selected using puromycin.

Western blot analysis

Cells were harvested as described previously.[41] Primary antibody incubation was performed overnight at 4 °C using the appropriate antibodies. Thereafter, blots were incubated with horseradish peroxidase-conjugated secondary antibody (GE Healthcare, Diegem, The Netherlands) in tris buffered saline-tween (tBS-T) for 1 h at room temperature. Protein signals were detected with ECL-plus method (GE Healthcare) followed by scanning of the blots with a Typhoon 9400 (GE Healthcare).

Animals

Female 12-week-old Rag2$^{-/-}$ γc$^{-/-}$ mice were obtained from in-house breeding. Animals were housed in individually ventilated cages under sterile conditions. Housing and experiments were performed according to the Dutch guidelines for the care and use of laboratory animals (UL-DEC-6117). Sterilized food and water were provided *ad libitum*.

In vivo tumor growth and metastasis formation of MDA-MB-231 cells

A total of 5×10^5 MDA-MB-231 LM2 cells in 0.1 ml phosphate-buffered saline were injected into the fat pad of Rag2$^{-/-}$ γc$^{-/-}$ mice ($n = 7$). Size of the primary tumors was measured by using calipers. Animals were anesthetized when tumor volume reached $7 \times 7\,mm^2$ and primary tumor was removed. Lung metastasis formation was followed over time using bio-luminescent imaging. At 17–21 days after primary tumor removal, mice were killed and lung metastasis was determined using bio-luminescent imaging (total lung burden) and live imaging of GFP (individual lung mets) using confocal laser scanning microscopy. See Supplementary Materials and methods for details. All animal experiments were approved by the local ethical committee.

In vivo tumor growth and metastasis formation of MTLn3 cells

A total of 2×10^5 MTLn3 cells in 0.1 ml phosphate-buffered saline were injected into the fat pad of Rag2$^{-/-}$ γc$^{-/-}$ mice. After the fat pad injection, the size of the primary tumors was measured by using calipers. Animals were anesthetized at indicated time points with Nembutal and the primary tumor and lungs were excised. The right lung was injected with ink solution and thereafter destained in water and fixated in Feketes (4.3% (v/v) acetic acid, 0.35% (v/v) formaldehyde in 70% ethanol). Surface lung metastases were counted for each animal ($n = 5$–7 per group). All animal experiments were approved by the local ethical committee.

Immunohistochemistry

Tumors and lungs were embedded in paraffin and sectioned (4 μm) onto 3-aminopropyltriethoxysilane-coated slides. After deparaffinization, the tumor and lung sections were stained for hematoxylin/eosin and lungs were examined for lung metastasis formation. The number of lung metastasis per paraffin section was counted. Paraffin sections were deparaffinized, followed by antigen retrieval in citrate buffer, incubation with primary (AnxA2, ki67) and alexa-488 secondary antibodies.

Statistical analysis *in vitro* and *in vivo*

Tissue microarray statistical analysis was done using Statistical Package for the Social Sciences SPSS 15.0 (SPSS, Inc., IBM Nederland, Amsterdam, The Netherlands) and differences in proportions were tested by Pearson χ^2. For *in vitro* and *in vivo* animal studies, Student's *t*-test was used to determine if there was a significant difference between two means ($P < 0.05$). When multiple means were compared, significance was determined by one-way analysis of variance ($P < 0.05$). Significant differences are marked in the graphs.

ABBREVIATIONS

AnxA1, Annexin A1; AnxA2, Annexin A2; ER, estrogen receptor; EGF, epidermal growth factor; EGFR, epidermal growth factor receptor; GFP, green fluorescent protein; RNAi, RNA interference; shRNA, small hairpin RNA; TNBC, triple negative breast cancer; WT, wild type

CONFLICT OF INTEREST

The authors declare no conflict of interest.

ACKNOWLEDGEMENTS

We thank Dr Erik Danen and Dr Leo Price for critically reading the manuscript. This work was supported by grants from the Dutch Cancer Society (KWF; grant UL 2006-3538 and UL 2007-3860), EU FP7-Metafight (grant no 201862), EUFP7 Systems Microscopy NoE (258068), TI Pharma project T3-107, the Dutch Organization for Scientific Research (NWO 911-02-022), Horizon Breakthrough (NWO 93518003) and Centre for Biomedical Genetics.

REFERENCES

1 Eccles SA. The epidermal growth factor receptor/Erb-B/HER family in normal and malignant breast biology. *Int J Dev Biol* 2011; **55**: 685–696.
2 Badovinac-Crnjevic T, Jakic-Razumovic J, Podolski P, Plestina S, Sarcevic B, Munjas R *et al.* Significance of epidermal growth factor receptor expression in breast cancer. *Med Oncol* 2011; **28**(Suppl 1): S121–S128.
3 Grandal MV, Madshus IH. Epidermal growth factor receptor and cancer: control of oncogenic signalling by endocytosis. *J Cell Mol Med* 2008; **12**: 1527–1534.
4 Geldner N, Jurgens G. Endocytosis in signalling and development. *Curr Opin Plant Biol* 2006; **9**: 589–594.
5 Murphy JE, Padilla BE, Hasdemir B, Cottrell GS, Bunnett NW. Endosomes: a legitimate platform for the signaling train. *Proc Natl Acad Sci USA* 2009; **106**: 17615–17622.
6 Jiang X, Huang F, Marusyk A, Sorkin A. Grb2 regulates internalization of EGF receptors through clathrin-coated pits. *Mol Biol Cell* 2003; **14**: 858–870.
7 Waterman H, Levkowitz G, Alroy I, Yarden Y. The RING finger of c-Cbl mediates desensitization of the epidermal growth factor receptor. *J Biol Chem* 1999; **274**: 22151–22154.
8 Mosesson Y, Mills GB, Yarden Y. Derailed endocytosis: an emerging feature of cancer. *Nat Rev Cancer* 2008; **8**: 835–850.
9 Cao L, Yan K, Winkel L, de Graauw M, Verbeek FJ. Pattern recognition in high-content cytomics screens for target discovery. *Proceedings of the 6th IAPR International Conference on Pattern Recognition in Bioinformatics*. Springer-Verlag:: Berlin2012: pp 330–342, .
10 Grieve AG, Moss SE, Hayes MJ. Annexin A2 at the interface of actin and membrane dynamics: a focus on its roles in endocytosis and cell polarization. *Int J Cell Biol* 2012; **2012**: 852430.
11 de Graauw M, van Miltenburg MH, Schmidt MK, Pont C, Lalai R, Kartopawiro J *et al.* Annexin A1 regulates TGF-beta signaling and promotes metastasis formation of basal-like breast cancer cells. *Proc Natl Acad Sci USA* 2010; **107**: 6340–6345.
12 Minn AJ, Gupta GP, Padua D, Bos P, Nguyen DX, Nuyten D *et al.* Lung metastasis genes couple breast tumor size and metastatic spread. *Proc Natl Acad Sci USA* 2007; **104**: 6740–6745.
13 Sharma MR, Koltowski L, Ownbey RT, Tuszynski GP, Sharma MC. Angiogenesis-associated protein annexin II in breast cancer: selective expression in invasive breast cancer and contribution to tumor invasion and progression. *Exp Mol Pathol* 2006; **81**: 146–156.
14 de Graauw M, Tijdens I, Smeets MB, Hensbergen PJ, Deelder AM, van de Water B. Annexin A2 phosphorylation mediates cell scattering and branching morphogenesis via cofilin Activation. *Mol Cell Biol* 2008; **28**: 1029–1040.
15 Okreglak V, Drubin DG. Cofilin recruitment and function during actin-mediated endocytosis dictated by actin nucleotide state. *J Cell Biol* 2007; **178**: 1251–1264.
16 Llado A, Timpson P, Vila de MS, Moreto J, Pol A, Grewal T *et al.* Protein kinase Cdelta and calmodulin regulate epidermal growth factor receptor recycling from early endosomes through Arp2/3 complex and cortactin. *Mol Biol Cell* 2008; **19**: 17–29.
17 Marcoux N, Vuori K. EGF receptor activity is essential for adhesion-induced stress fiber formation and cofilin phosphorylation. *Cell Signal* 2005; **17**: 1449–1455.
18 Miyamoto Y, Yamauchi J, Itoh H. Src kinase regulates the activation of a novel FGD-1-related Cdc42 guanine nucleotide exchange factor in the signaling pathway from the endothelin A receptor to JNK. *J Biol Chem* 2003; **278**: 29890–29900.
19 Richnau N, Aspenstrom P. Rich, a rho GTPase-activating protein domain-containing protein involved in signaling by Cdc42 and Rac1. *J Biol Chem* 2001; **276**: 35060–35070.
20 Pepinsky RB, Sinclair LK. Epidermal growth factor-dependent phosphorylation of lipocortin. *Nature* 1986; **321**: 81–84.
21 Vila de MS, Timpson P, Cubells L, Evans R, Hayes TE, Rentero C *et al.* Annexin A6 inhibits Ras signalling in breast cancer cells. *Oncogene* 2009; **28**: 363–377.
22 Grewal T, Koese M, Rentero C, Enrich C. Annexin A6-regulator of the EGFR/Ras signalling pathway and cholesterol homeostasis. *Int J Biochem Cell Biol* 2010; **42**: 580–584.
23 Croxtall JD, Choudhury Q, Flower RJ. Glucocorticoids act within minutes to inhibit recruitment of signalling factors to activated EGF receptors through a receptor-dependent, transcription-independent mechanism. *Br J Pharmacol* 2000; **130**: 289–298.
24 White IJ, Bailey LM, Aghakhani MR, Moss SE, Futter CE. EGF stimulates annexin 1-dependent inward vesiculation in a multivesicular endosome subpopulation. *EMBO J* 2006; **25**: 1–12.
25 Emoto K, Yamada Y, Sawada H, Fujimoto H, Ueno M, Takayama T *et al.* Annexin II overexpression correlates with stromal tenascin-C overexpression: a prognostic marker in colorectal carcinoma. *Cancer* 2001; **92**: 1419–1426.
26 Zheng L, Foley K, Huang L, Leubner A, Mo G, Olino K *et al.* Tyrosine 23 phosphorylation-dependent cell-surface localization of annexin A2 is required for invasion and metastases of pancreatic cancer. *PLoS One* 2011; **6**: e19390.
27 Wu B, Zhang F, Yu M, Zhao P, Ji W, Zhang H *et al.* Up-regulation of Anxa2 gene promotes proliferation and invasion of breast cancer MCF-7 cells. *Cell Prolif* 2012; **45**: 189–198.
28 Jost M, Zeuschner D, Seemann J, Weber K, Gerke V. Identification and characterization of a novel type of annexin-membrane interaction: Ca2+ is not required for the association of annexin II with early endosomes. *J Cell Sci* 1997; **110**(Pt 2): 221–228.
29 Harder T, Gerke V. The subcellular distribution of early endosomes is affected by the annexin II2p11(2) complex. *J Cell Biol* 1993; **123**: 1119–1132.
30 Mayran N, Parton RG, Gruenberg J. Annexin II regulates multivesicular endosome biogenesis in the degradation pathway of animal cells. *EMBO J* 2003; **22**: 3242–3253.
31 Shetty PK, Thamake SI, Biswas S, Johansson SL, Vishwanatha JK. Reciprocal regulation of annexin A2 and EGFR with Her-2 in Her-2 negative and herceptin-resistant breast cancer. *PLoS One* 2012; **7**: e44299.
32 Goswami S, Sahai E, Wyckoff JB, Cammer M, Cox D, Pixley FJ *et al.* Macrophages promote the invasion of breast carcinoma cells via a colony-stimulating factor-1/epidermal growth factor paracrine loop. *Cancer Res* 2005; **65**: 5278–5283.
33 Le Devedec SE, van RW, Maria N, Grimbergen M, Pont C, Lalai R *et al.* An improved model to study tumor cell autonomous metastasis programs using MTLn3 cells and the Rag2(−/−) gammac (−/−) mouse. *Clin Exp Metastasis* 2009; **26**: 673–684.
34 Babbin BA, Parkos CA, Mandell KJ, Winfree LM, Laur O, Ivanov AI *et al.* Annexin 2 regulates intestinal epithelial cell spreading and wound closure through Rho-related signaling. *Am J Pathol* 2007; **170**: 951–966.
35 Rescher U, Ludwig C, Konietzko V, Kharitonenkov A, Gerke V. Tyrosine phosphorylation of annexin A2 regulates Rho-mediated actin rearrangement and cell adhesion. *J Cell Sci* 2008; **121**: 2177–2185.
36 Nishimura Y, Yoshioka K, Bernard O, Bereczky B, Itoh K. A role of LIM kinase 1/cofilin pathway in regulating endocytic trafficking of EGF receptor in human breast cancer cells. *Histochem Cell Biol* 2006; **126**: 627–638.
37 Wang W, Eddy R, Condeelis J. The cofilin pathway in breast cancer invasion and metastasis. *Nat Rev Cancer* 2007; **7**: 429–440.
38 Sidani M, Wessels D, Mouneimne G, Ghosh M, Goswami S, Sarmiento C *et al.* Cofilin determines the migration behavior and turning frequency of metastatic cancer cells. *J Cell Biol* 2007; **179**: 777–791.
39 Huigsloot M, Tijdens IB, Mulder GJ, van de Water B. Differential regulation of doxorubicin-induced mitochondrial dysfunction and apoptosis by Bcl-2 in mammary adenocarcinoma (MTLn3) cells. *J Biol Chem* 2002; **277**: 35869–35879.
40 Lombaerts M, van WT, Philippo K, Dierssen JW, Zimmerman RM, Oosting J *et al.* E-cadherin transcriptional downregulation by promoter methylation but not mutation is related to epithelial-to-mesenchymal transition in breast cancer cell lines. *Br J Cancer* 2006; **94**: 661–671.
41 de Graauw M, Tijdens I, Cramer R, Corless S, Timms JF, van de Water B. Heat shock protein 27 is the major differentially phosphorylated protein involved in renal epithelial cellular stress response and controls focal adhesion organization and apoptosis. *J Biol Chem* 2005; **280**: 29885–29898.
42 van Roosmalen W, Le Devedec SE, Zovko S, de BH, van de WB. Functional screening with a live cell imaging-based random cell migration assay. *Methods Mol Biol* 2011; **769**: 435–448.

Supplementary Information accompanies this paper on the Oncogene website (http://www.nature.com/onc)